

Development and Comparative Analysis of Chaos Diagram for Harmonically Excited Duffing Oscillator Using Gram-Schmidt Orthogonal Based Lyapunov Exponent

Toluwalope J. John , Tajudeen A.O. Salau, Daniel O. Ayegbeso, Azeez A. Adebayo

Mechanical Engineering
University of Ibadan
Nigeria

Corresponding author email: johntoluwalopejoshua@gmail.com

Abstract

The motivation for this work is the development of a reliable alternative and laboratory relevant chaos diagrams for excited Duffing oscillators. A Gram Schmidt Orthogonal-based Lyapunov exponent was utilized to indicate points as well as regions characterized by periodic or chaotic motion for the harmonically excited Duffing oscillator. A graphical collection of chaotically behaving points called chaos diagram was developed for the choice drive parameter combinations on the plane ($0.07 \leq \omega \leq 1.5$ and $0.07 \leq P \leq 1.5$). Specific cases that were studied include the three equilibria $(-1,0)$, $(0,0)$ and $(1,0)$ as initial conditions and two damped levels 0.168 and 0.0168. Different resolutions studied, give an average of 28.4% of parameter combination points that makes the system behave chaotically. In addition, the percentage of the parameter points behaving chaotically increases significantly with a decrease in the damp coefficient for each of the equilibrium positions. Initial condition $(0,0)$ with damped coefficients 0.168 and 0.0168 resulted in 28.7% and 90.6 % chaotically behaving points respectively while initial condition $(1,0)$ with damped coefficients 0.168 and 0.0168 produced 28.6% and 88.9 % chaotically behaving points respectively. In addition, for initial condition $(-1,0)$ with damped coefficients 0.168 and 0.0168 percentage of chaotically behaving points are 29.5% and 88.9% respectively. The chaos diagram generated in this paper can be utilized in the lab to rapidly and accurately identify the driving parameter combination that causes the Duffing oscillator to behave chaotically or periodically under harmonic excitation.

Keywords: Nonlinear Vibration, Chaos, Duffing Oscillator, Orthogonalization,

Date of Submission: 08-07-2022

Date of Acceptance: 22-07-2022

I. Introduction

Nature is fundamentally nonlinear, which explains why natural systems have such a wide range of capabilities[1]. Many engineering systems are motivated by nature's behavior, and research into developing appropriate methods to understand nonlinear systems is being conducted. Stability is a crucial problem in nonlinear dynamical systems, as it is linked to the characteristics of a solution that has been perturbed. The system is stable if a perturbation has no noticeable effect on its response. Aside from that, the device is insecure. When contemplating the movement of a body, there are in three different scenarios of the body being in equilibrium namely; unstable, stable and neutral equilibrium. Stability establishes a link between a dynamical system's orbit or solution and its perturbation, which is characterized by an adjacent orbit with a different starting condition than the original. Lyapunov's stability definition describes a stable system as one in which two nearby orbits remain close to each other as time passes [2].The responses of nonlinear dynamical systems are extremely diverse. This can be thought of as a type of device independence that is linked to alternative behaviors. Chaos is one of these possibilities connected with variety and unpredictability. In a nutshell, chaos is defined as deterministic nonlinear systems that exhibit bounded random-like behavior and are sensitive to initial condition[3]. The terms "random" and "chaotic" motions must be distinguished here. The former is for problems when we don't have a thorough understanding of the input forces or only have statistical measurements of the parameters.The word chaotic refers to deterministic situations without any random or unexpected inputs or parameters. Chaotic system is characterized by a sensitive dependency on initial conditions, and has a range of responses including aperiodic, periodic and chaotic.Chaos is a nonscientific concept that has been around for a

long time, and it is frequently linked to a bodily condition or out-of-control human conduct. Turbulence is the epitome of chaotic occurrences in the physical sciences. The idea that the transition from ordered to disordered flow can be explained or predicted using relatively basic mathematical equations is at the heart of today's nonlinear dynamics thrill. Poincare was aware that classical physics equations may produce chaotic or unpredictable motions [4]. Poincare had a crystal clear view of chaos (as we understand it today), but it wasn't until 1963, when Lorenz performed meteorology studies, that this idea returned to the scientific scenario [5]. The butterfly effect, which states that if a butterfly flaps its wings in China, it may trigger a hurricane in Brazil, was established through Lorenz's investigation [2]. Despite the fact that [6], [7], [8], and [9] referred to such irregular behavior of nonlinear systems in their seminal works, a systematic analysis of chaos has only been carried out in the last two decades, aided by the vast computing power offered by modern computers and sophisticated graphic facilities [3]. Non-linear oscillations are inextricably linked to the Duffing equation, often known as the Duffing oscillator. The Duffing oscillator is also thought to be a prototype for nonlinear dynamics systems. The Duffing-type equation is a mathematical model of motion of a single-degree-of-freedom system with linear or nonlinear damping and nonlinear stiffness, such as a mass hanging on a parallel combination of a constant damping dashpot and a nonlinear restoring force, activated by a harmonic force [10]. Non-linear oscillations offer a wide range of important and interesting applications [11], which is not surprising, given that the traditional methods for tackling such non-linear problems are well-known today, and that in non-linear oscillations, new and very abstract mathematical tools develop in a natural way. Chaos in Duffing type nonlinear oscillators has gotten a lot of attention [12]. The term "chaotic" identifies a set of motions in deterministic physical and mathematical systems whose temporal history is heavily influenced by initial conditions [4]. The Lyapunov exponent, which is a measure of the system's sensitivity to beginning circumstances, is the most precise approach to quantify chaos. [5], [13], [14] demonstrated that under certain initial conditions, a nonlinear harmonically stimulated system (e.g a Duffing oscillator) will behave chaotically or periodically. The combination of the drive parameters determines the stochastic behavior. There have been chaotic diagrams created from prior studies using other tools, but none employing the Gram Schmidt orthogonal based Lyapunov exponent. Using a Gram Schmidt orthogonal based Lyapunov exponent numerical technique, this article aims to fill such gap in the literature.

II. Methodology

The project research method involves computer simulation. The programming language that was used to carry out the simulation was Python programming language on a laptop with the following properties: processor (Intel(R) Core(TM) i5-2520M CPU @ 2.50GHz 2.50 GHz), RAM (4GB) and 64-bit operating system.

The desired results were achieved in the following process;

- Solving the transformed Duffing equation using Runge kutta fourth order scheme for a constant time step to give the displacement and velocity for each time step.
- The displacement obtained from the non-linear Duffing using Runge Kutta fourth order subroutine was then used to evaluate the linear system of the Lyapunov coordinates for each time step.
- The coordinates of the Lyapunov coordinates obtained was orthonormalized after a specified number of steps using Gram-schmidt Orthonormalization method.
- The magnitude of the orthogonal Lyapunov vectors was used to evaluate the Lyapunov exponent. The rate of divergence of two neighboring trajectories is measured by the Lyapunov exponent. A positive value of Lyapunov exponent depicts chaos while a negative Lyapunov exponent indicates no chaos.
- A chaos diagram is developed for each of the points for the parameter combinations (force amplitude and damping frequency)

2.1 DUFFING OSCILLATOR

Duffing's conventional equation is as follows::

$$\ddot{x} + \delta\dot{x} + \alpha x + \beta x^3 = P_o \sin \omega t \tag{1}$$

Where δ is the damping coefficient, α and β are stiffness (restoring) coefficients, P_o is the coefficient of excitation, ω is the frequency of excitation and t is the time [15].

From equation (1), a normalized governing equation for the dynamic behavior of a harmonically excited Duffing system was developed (2).

$$\ddot{x}_1 + \delta\dot{x}_1 - \frac{x_1}{2}(1 - x_1^2) = P_o \sin \omega t \tag{2}$$

Let x_1 and x_2 be displacement and velocity respectively. Then, equation (2) transformed to a pair of first order differential equation as given in equations (3) and (4).

$$\dot{x}_1 = x_2 = f_1 \tag{3}$$

$$\dot{x}_2 = P_o \cos \omega t - (\delta x_2 - \frac{x_1}{2}(1 - x_1^2)) = f_2 \tag{4}$$

2.2 RUNGE KUTTA FOURTH ORDER SCHEME

Equations (3) and (4) were simulated using Runge Kutta fourth order scheme for a constant time step (h) as given in equations 5-9. Worthy of note is that there are different coefficients utilized in Runge Kutta fourth order which is not limited to equation 5-9 alone [13].

$$K_1 = f(x_i, y_i) \tag{5}$$

$$K_2 = f(x_i + \frac{h}{2}, y_i + \frac{hK_1}{2}) \tag{6}$$

$$K_3 = f(x_i + \frac{h}{2}, y_i + \frac{hK_2}{2}) \tag{7}$$

$$K_4 = f(x_i + h, y_i + hK_3) \tag{8}$$

$$y_{i+1} = y_i + \frac{h}{6}(K_1 + 2(K_2 + K_3) + K_4) \tag{9}$$

2.3 STUDIED CASE PARAMETER DETAILS

A case under investigation was defined as a parameter point in the parameter space. Different resolutions were examined for different excitation frequency (ω) and force amplitude (P_o) combinations with the drive parameters range given as $0.07 \leq \omega \leq 1.5$ and $0.07 \leq P_o \leq 1.5$ respectively as well as two damping levels ($\gamma = 0.168$ and $\gamma = 0.0168$). The simulation time step was fixed at $h = T_p/500$ for $T_p = 2\pi/\omega$ and the initial conditions for displacement and velocity for studied cases are (0, 0), (1, 0), (-1, 0). Due to the problem of long computation time the simulation was executed for 10 steady cycles (i.e. $10T_p$ to $20T_p$). T_p and h are period and time step respectively while other parameters used in subsequent sections are N_{start} = Numbers of runaway cycles, N_{end} = Total number of cycles for the entire simulation.

2.4 JACOBIAN

The initial partial derivatives of the same function with respect to each of the variables in each row make up the Jacobian, which is defined for a finite number of functions with the same number of variables. The Jacobian matrix, or simply Jacobian, is a matrix used to convert surface and volume integrals from one coordinate system to the next. [16].

The displacement obtained from the non-linear Duffing using Runge Kutta fourth order subroutine was utilized by the Jacobian operation on equations (3) and (4) as shown in equation (10) [17] used to evaluate the linear system of the Lyapunov coordinates for each time step.

The functions f_1 and f_2 are as provided in equations 3 and 4.

$$J = \begin{bmatrix} \frac{\partial f_1}{\partial x_1} & \frac{\partial f_1}{\partial x_2} \\ \frac{\partial f_2}{\partial x_1} & \frac{\partial f_2}{\partial x_2} \end{bmatrix} = \begin{bmatrix} 0 & 1 \\ 0.5 - 1.5x_1^2 & -\delta \end{bmatrix} \tag{10}$$

A pair of first order equations is derived with the Jacobian

$$\begin{Bmatrix} \dot{\tau}_1 \\ \dot{\tau}_2 \end{Bmatrix} = J \begin{Bmatrix} \tau_1 \\ \tau_2 \end{Bmatrix} = \begin{bmatrix} 0 & 1 \\ 0.5 - 1.5x^2 & -\delta \end{bmatrix} \begin{Bmatrix} \tau_1 \\ \tau_2 \end{Bmatrix} \tag{11}$$

Equation (11) was evaluated using Runge Kutta fourth order as explained in section (2.2)

2.5 GRAM SCHMIDT ORTHONORMALIZATION

The Gram-Schmidt method works by removing orthogonal projections from vectors in a sequential manner. One of the most important applications of the inner product is the projection operator, which we will now define.

A projection operator is defined by

$$proj_u(v) = \frac{\langle u, v \rangle}{\langle u, u \rangle} u$$

The inner product of the vectors u and v is denoted by $\langle u, v \rangle$. This operator orthogonally projects the vector v onto the line spanned by vector u . We define $proj_0(v) = 0$, if $u = 0$, i.e., the projection map $proj_0$ is the zero map, sending every vector to the zero vector. [18]

The Gram-Schmidt procedure then goes like this::

$$u_1 = v_1 \qquad e_1 = \frac{u_1}{\|u_1\|}$$

$$u_2 = v_2 - proj_{u_1}(v_2) \qquad e_2 = \frac{u_2}{\|u_2\|}$$

$$u_3 = v_3 - proj_{u_1}(v_3) - proj_{u_2}(v_3) \qquad e_3 = \frac{u_3}{\|u_3\|}$$

$$u_4 = v_4 - \text{proj}_{u_1}(v_4) - \text{proj}_{u_2}(v_4) - \text{proj}_{u_3}(v_4)e_3 = \frac{u_3}{\|u_3\|}$$

.....

.....

$$u_k = v_k - \sum_{j=1}^{k-1} \text{proj}_{u_j}(v_k)$$

$$e_k = \frac{u_k}{\|u_k\|}$$

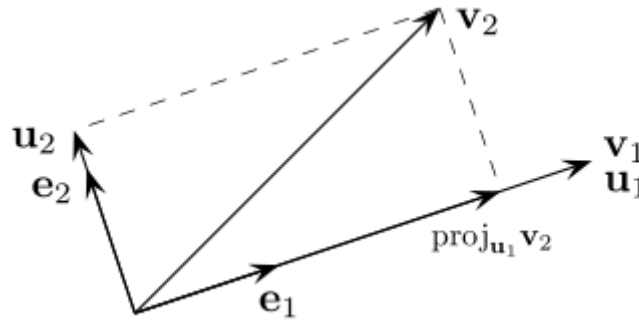


Fig 2.1 .First two steps of Gram-Schmidt process(William, 2015)

2.6 LYAPUNOV EXPONENT

Lyapunov exponents are related to the expanding and contracting nature of distinct orientations in phase space. According to [19], a continuous technique is straightforward and dependable for computing the complete or partial Lyapunov spectrum associated with a dynamical system specified by a set of differential equations. The relationship between the original D-sphere and the D-ellipsoid is used to evaluate the divergence of two adjacent orbits as shown in fig (2.2)[2].

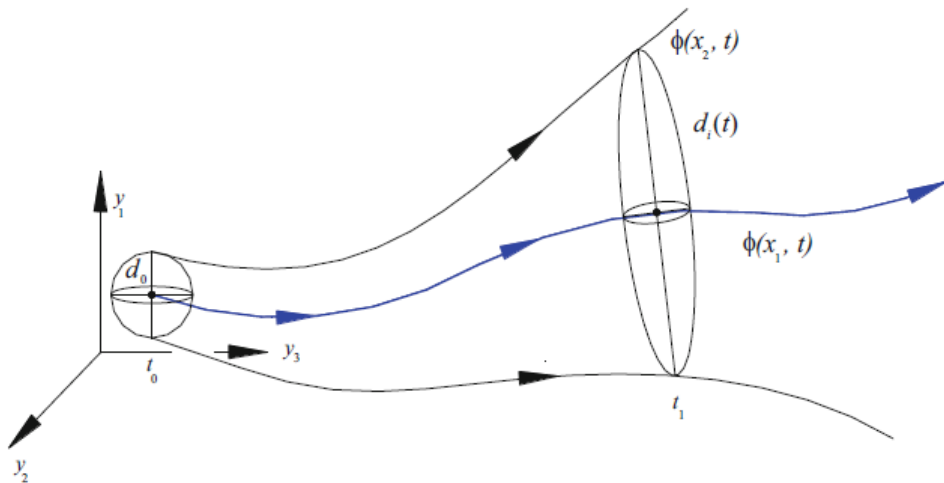


Fig 2.2 Lyapunov exponent(Savi, 2017)

This variation may be expressed by:

$$d(t) = d_0 b^{\lambda t}$$

Where $d(t)$, b , λ is the diameter, reference basis, Lyapunov exponent respectively. Hence, the Lyapunov spectrum can be given by:

$$\lambda = \frac{1}{t} \log_b \frac{d(t)}{d_0}$$

III. Result And Discussion

3.1 VALIDATION OF CODE USING PUBLISHED PHASE PLOTS AND POINCARÉ RESULTS

Comparison was done for the phase plane trajectory and Poincaré sections under harmonic excitation. The phase plane trajectory and Poincaré patterns compare excellently well with those reported by [5] for the five cases as shown in the figures 3.1-3.5.

Note: Initial condition of $(x_1, x_2) = (0,0)$, $\gamma = 0.168$ and $\omega = 1$ are common to figures 3.1-3.4. While $(x_1, x_2) = (0,0)$ and $\gamma = 0.0168$, $\omega = 1$ applies to figure 3.5.

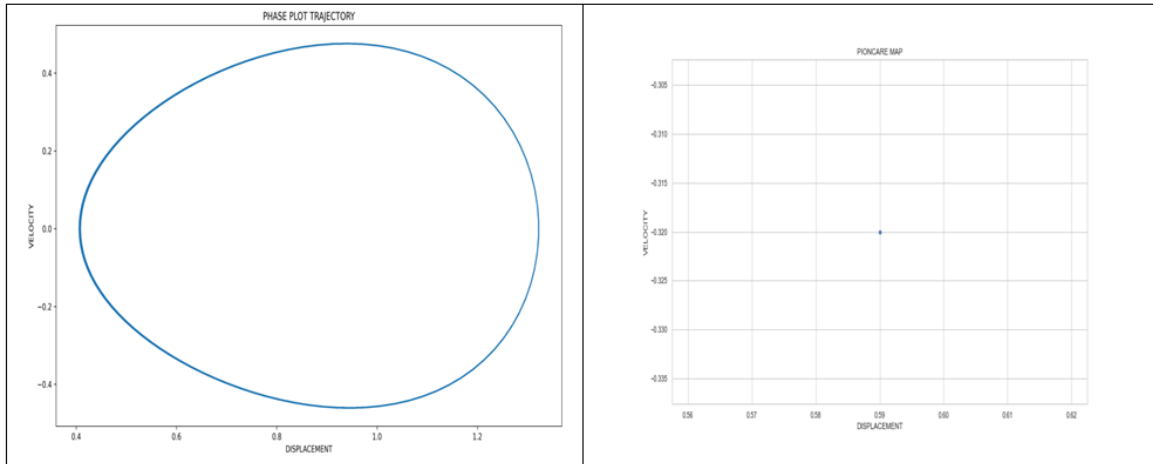


Figure 3.1: Phase plot and its corresponding Poincaré for case-1 at $(P_0=0.177)$

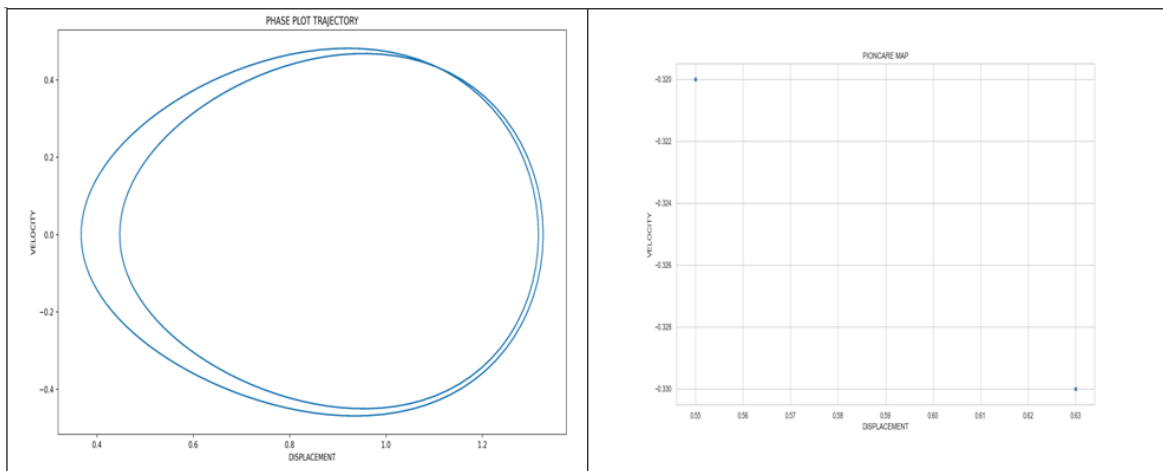


Figure 3.2: Phase plot and its corresponding Poincaré for case-2 at $(P_0=0.178)$

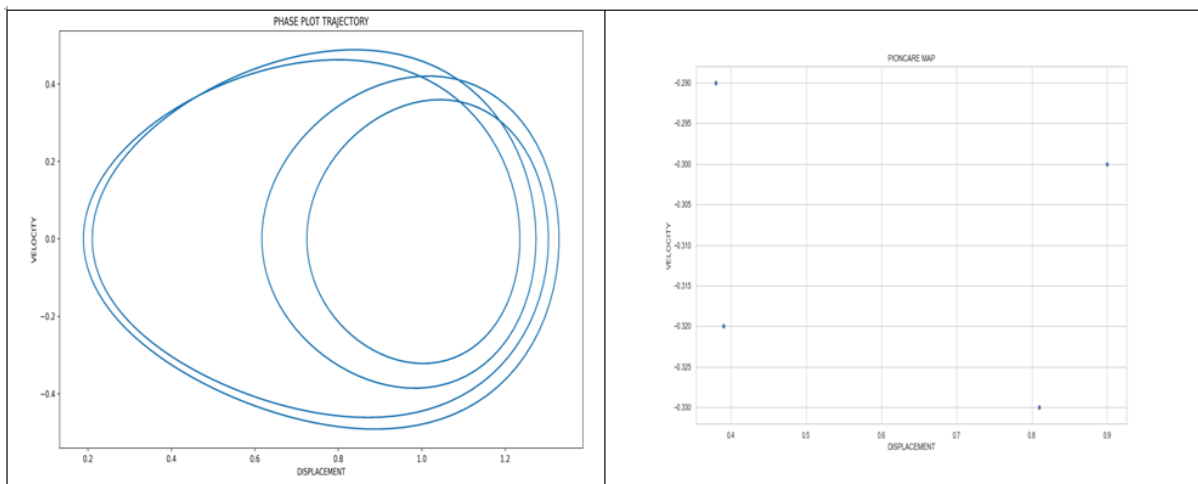


Figure 3.3: Phase plot and its corresponding Poincaré for case-3 at $(P_0=0.197)$

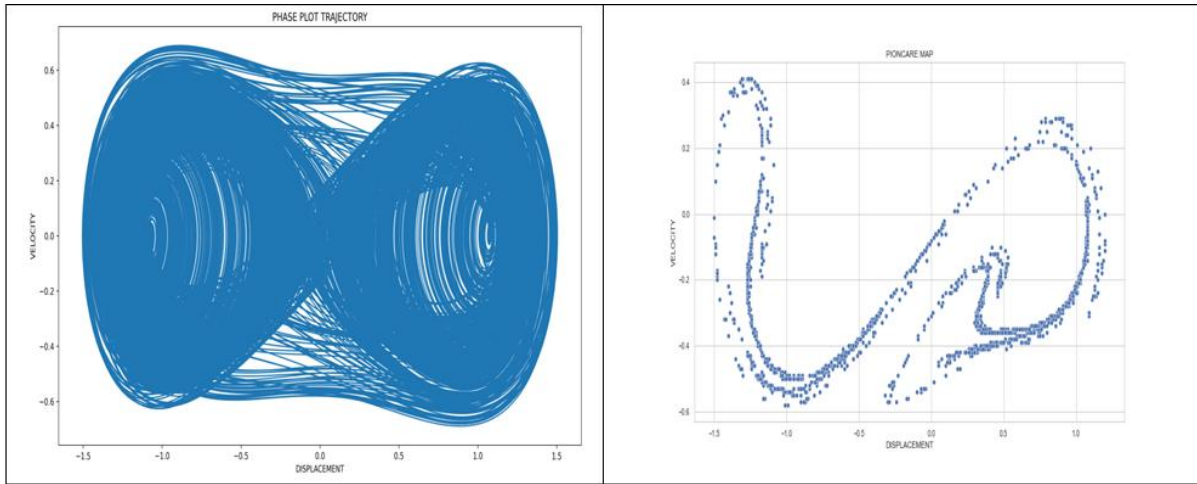


Figure 3.4: Phase plot and its corresponding Poincare for case-4 at ($P_o=0.21$)

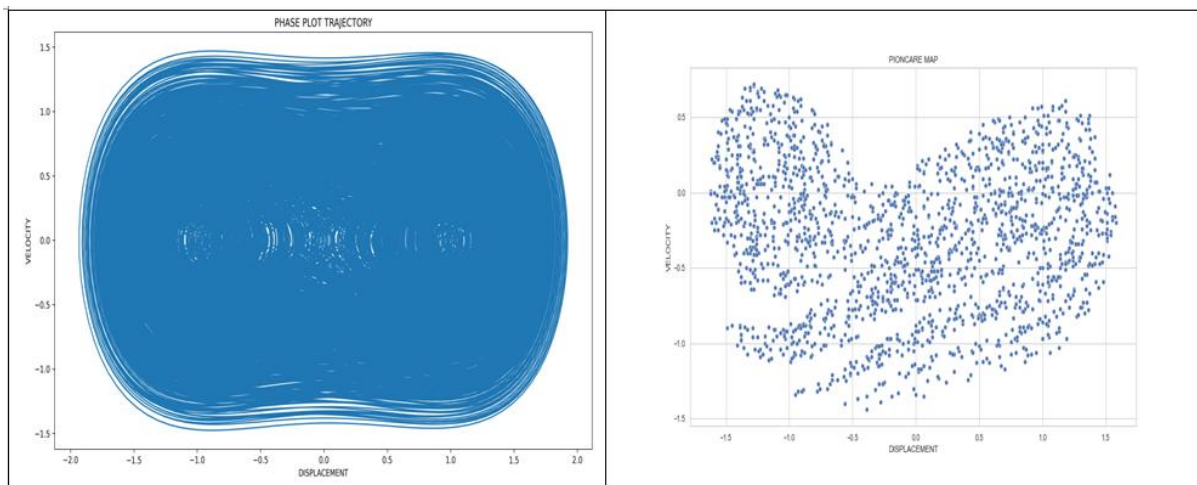


Figure 3.5: Phase plot and its corresponding Poincare for case-5 at ($P_o=0.19, \gamma = 0.0168$)

3.2 VALIDATION OF CODES FOR ESTIMATING LYAPUNOV EXPONENTS IN COMPARISON TO PUBLISHED PHASE PLOT AND POINCARÉ RESULTS

The initial conditions used in the simulation to get the result in Table(3.1) as required in the code is given below

Initial displacement and velocity $(x_1, x_2) = (0, 0)$

Initial conditions for Lyapunov coordinates $(lx_0, ly_0), lx_1, ly_1) = (1, 0), (0, 1)$

$N_{start}, N_{end} = 200, 2000$

N_{slice} per period of forcing frequency = 100

$N_{count} = 10$

Table 3.1

CASES	DESCRIPTION	LYAPUNOV EXPONENT 1	LYAPUNOV EXPONENT 2	Remarks
1	1 periodic motion	-0.003	-0.165	Periodic
2	2 periodic motion	-0.007	-0.161	Periodic
3	4 periodic motion	-0.084	-0.084	Periodic
4	Chaotic motion	0.102	-0.270	Chaotic
5	Chaotic motion	0.143	-0.160	Chaotic

Comparing the remark with the corresponding cases with their counterpart Figure 3.1-3.5, the method of Lyapunov exponents characterization agrees to the phase plot and Poincaré map as reported by [5].

3.3 DEVELOPMENT OF CHAOS DIAGRAM

Drive parameters used in developing the chaos diagram are given as $(0.07 < P_o < 1.5), (0.07 < \omega < 1.5), (x_1, x_2) = (0, 0)$ or $(1, 0)$ or $(-1, 0), \gamma = 0.168$ and 0.0168 .

3.3.1 Choice of cycles to carry out simulation

The simulation that gave the result in Table 3.2 has the following drive parameters and initial conditions

1. $0.07 < P_0 < 1.5$
2. $0.07 < \omega < 1.5$
3. $(x_1, x_2) = (0,0)$
4. Initial condition for Lyapunov coordinates (1,0),(0,1)
5. $h = T_p/500$

Table 3.2

S/N	N_{start}	N_{end}	Time(s)	Percentage of chaotically behaving points for the given parameter combination
1	10	20	1148	28.8
2	10	25	1582	28.2
3	10	30	2020	27.8
4	10	40	2798	27.3

Due to the constraint of long computation time used in a as shown in Table 3.2 with no qualitative difference in the chaos for the N_{start} and N_{end} combination, the choice of N_{start} and N_{end} used for the simulation to develop the chaos diagram are 10 and 25 respectively.

3.3.2 Choice of the resolution for the chaos diagram

The simulation that gave the result in Table 3.3 has the following drive parameters and initial conditions

1. $(x_1, x_2) = (0,0)$
2. Initial condition for Lyapunov coordinates (1,0),(0,1)
3. $h = T_p/500$
4. $N_{start}, N_{end} = 10,25$

Table 3.3

Force amplitude	Excitation frequency	Resolution	Damping coefficient	Percentage of chaotically behaving points for the given parameter combination
$0.07 < P_0 < 1.5$	$0.07 < \omega < 1.5$	26×26	0.168	29
$0.07 < P_0 < 1.5$	$0.07 < \omega < 1.5$	51×51	0.168	28.2
$0.07 < P_0 < 1.5$	$0.07 < \omega < 1.5$	101×101	0.168	28.2
$0.07 < P_0 < 1.5$	$0.07 < \omega < 1.5$	201×201	0.168	28.1

The percentage of the chaotic points for the different resolutions as shown in table 3.3 has no qualitative difference with a resolution of 26×26 as an exception which is coarse. Hence any of the resolution can be used to develop the chaos diagram. In this report the choice of resolution is 101×101 to have a well resolved chaos diagram.

3.3.3 Chaos diagram

The chaos diagrams developed below has the following drive parameters and initial conditions common to them while the initial conditions and damping coefficient varies as shown in each of the figure below.

Similar parameters;

1. $0.07 < P_0 < 1.5$
2. $0.07 < \omega < 1.5$
3. Initial condition for Lyapunov coordinates (1,0),(0,1)
4. Time step (h) = $T_p/500$
5. Resolution= 101×101

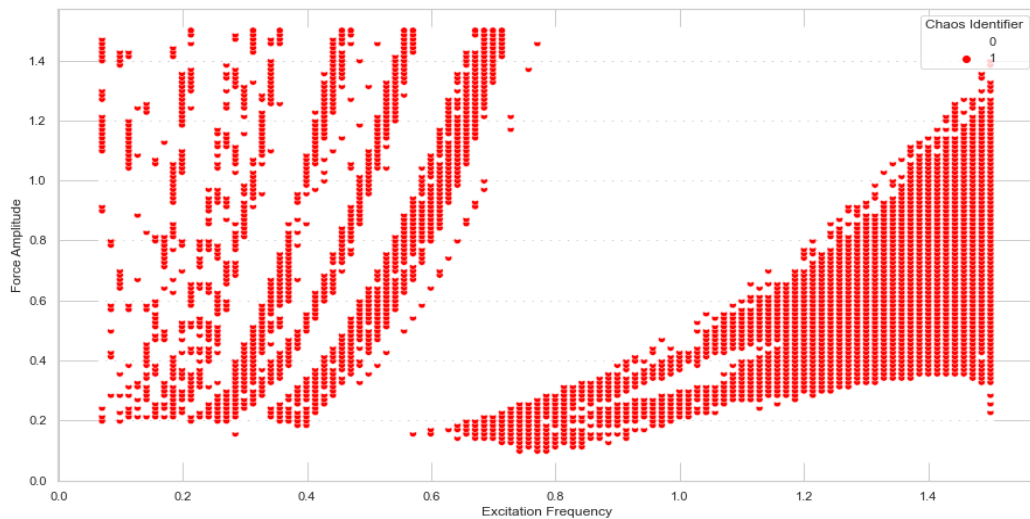


Figure 3.7: $(x_1, x_2) = (0, 0)$, $\gamma = 0.168$

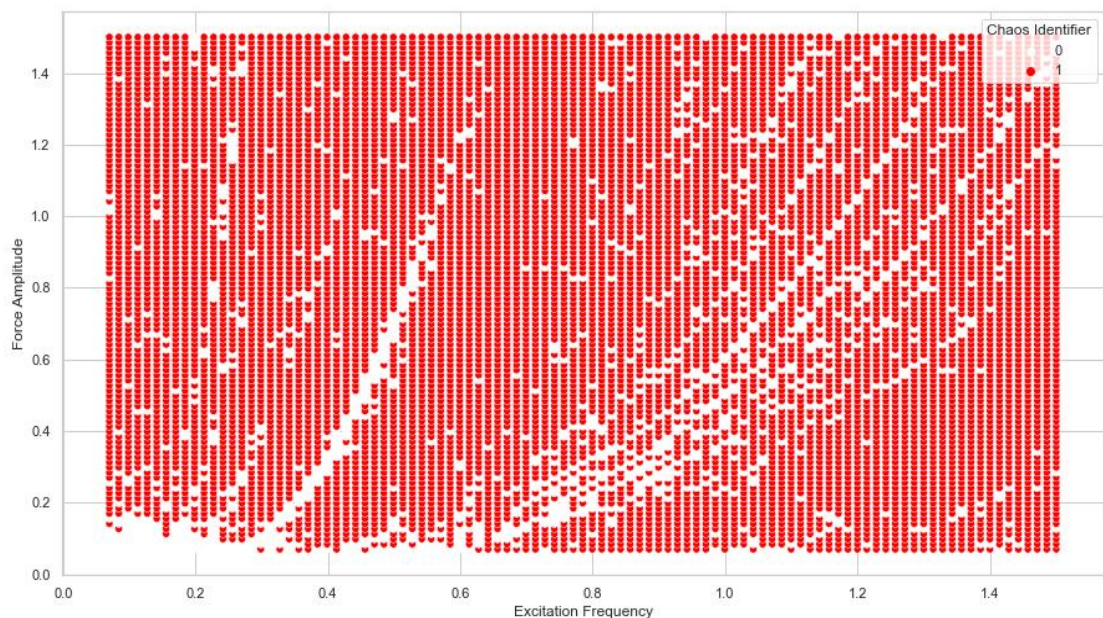


Figure 3.8: $(x_1, x_2) = (0, 0)$, $\gamma = 0.0168$

As reported by [20] when adaptive time steps were used, an optimum fractal disk dimension technique was used to characterize the produced weird attractor. Multiple trajectories of a harmonically excited Duffing oscillator are computed simultaneously using Runge-Kutta fourth and fifth order algorithms from relatively close initial conditions. Another study [14] used the fall to tolerance of absolute deviation between two independently sought solutions of the governing equation to classify Duffing oscillator excitation frequencies and amplitude parameter point as chaotic or not. In these two studies, a chaos diagram with the same parameter combination that gave the chaos diagram obtained in Figures 3.7 and 3.8 were developed. Therefore, the current chaos diagrams agrees with that reported in the two referenced studies thereby validating the tool Gram-Schmidt Orthogonal based Lyapunov exponent used in developing the chaos diagrams.

IV. Conclusion

In this study, chaos diagram for a harmonically excited Duffing oscillator has been developed with Gram-Schmidt orthonormalized Lyapunov exponent for the given drive parameters and the comparison of the chaos diagrams obtained conforms to that obtained in other published literature for the specific drive parameter combination which implies that the tool used is a reliable numerical tool in indicating the chaotic behavior of the deterministic Duffing oscillator. It can also be inferred that the three equilibrium positions for the oscillator has no significant qualitative and quantitative effect on the percentage of chaos for the same damping coefficient. The chaos diagram can be used as a chart in the lab to rapidly identify the drive parameter combination that will cause the system (Duffing oscillator) to act chaotically or periodically under harmonic excitation.

AUTHOR CONTRIBUTIONS

Toluwalope J. John reviewed relevant literatures and journals, wrote the research proposal, wrote an algorithm to simulate desired result, developed a chaos diagram and reported similar findings; Tajudeen A.O. Salau initiated the project and vetted the methods to ensure they were according to scientific standard; Daniel O. Ayegbeso reviewed relevant literatures and journals and contributed in developing the algorithm that were used in the simulation studies. The manuscript was written through the contribution of all authors. All authors discussed the results, reviewed, and approved the final version of the manuscript.

References

- [1]. Cuairan, M. T., Gieseler, J., Meyer, N., & Quidant, R. (2021), Precision calibration of the Duffing oscillator with phase control. 1, 1–6.
- [2]. Savi, M. A. (2017), Nonlinear dynamics and chaos nonlinear dynamics and chaos, <https://doi.org/10.1007/978-3-319-29982-2>
- [3]. Sekar, P., and Narayanan, S. (1995). Chaos in mechanical systems - A review. 20(August), 529–582.
- [4]. Moon, F. C. (2004). Chaotic Vibrations: An Introduction for Applied Scientists and Engineers, A John Wiley & sons, inc., publication.
- [5]. Dowell, E. . (1988). Chaotic oscillation in mechanical system (pp. 199–216).
- [6]. Poincare H 1921 The foundation of science: Science and method (New York: The Science Press)
- [7]. Birkhoff G. G. (1927), Dynamical systems, (Providence, RI: Am. Math. Soc.)
- [8]. Andronov A. A., Vitt A. A., Khaikin S. C. (1966), Theory of oscillators, (Oxford: Pergamon)
- [9]. Lyapunov A M 1949 Problème Général de la Stabilité du mouvement (Princeton: University Press)
- [10]. Wawrzynski, W. (2021). Duffing-type oscillator under harmonic excitation with a variable value of excitation amplitude and time-dependent external disturbances. Scientific Reports, 11(1), 1–15. <https://doi.org/10.1038/s41598-021-82652-z>
- [11]. Yamapi, R., and Orou, J. B. C. (2003), Harmonic oscillations , stability and chaos control in a non-linear electromechanical system. 259, 1253–1264. <https://doi.org/10.1006/jsvi.2002.5289>
- [12]. Dooren, R. Van. (1988). Behaviour in the duffing oscillator. 123, 327–339.
- [13]. Salau, T. A. O., Olaiya, K. A., and Ajide, O. O. (2014). Simulation of Oscillators Dynamics using Selected Versions of Fourth Order Runge-Kutta Scheme. 4(8), 444–454.
- [14]. Salau, T., and Ajide, O. (2012). Development of Chaos Diagrams for Duffing Oscillator Using Linearity and Nonlinearity Characteristics of Periodic and Chaotic Responses. International Journal of Engineering and ..., 2(9), 1529–1538. http://iet-journals.org/archive/2012/sep_vol_2_no_9/13621337813467.pdf
- [15]. Zeni, A. R., and Gallas, J. A. C. (1995). Lyapunov exponents for a Duffing oscillator. 89, 71–82.
- [16]. Rapp, B. E. (2017). Vector Calculus. Microfluidics: Modelling, Mechanics and Mathematics, 137–188. <https://doi.org/10.1016/b978-1-4557-3141-1.50007-1>
- [17]. Khatib, O. (2008). Introduction to robotics. (pp. 81–124).
- [18]. William, F. (2015). Gram-Schmidt Orthonormalization (pp. 281–297).
- [19]. Christianseny, F., and Rughz, H. H. . (1997), Computing Lyapunov spectra with continuous Gram - Schmidt orthonormalization Computing Lyapunov spectra with continuous Gram – Schmidt orthonormalization. 1063.
- [20]. Salau, T. A., and Ajide, O. (2012). Comparative Analysis of Time Steps Distribution in Runge Kutta algorithm. International Journal of Scientific and Engineering Research, 3(1), 1–5.

Toluwalope J. John, et. al. “Development and Comparative Analysis of Chaos Diagram for Harmonically Excited Duffing Oscillator Using Gram-Schmidt Orthogonal Based Lyapunov Exponent”. *IOSR Journal of Mechanical and Civil Engineering (IOSR-JMCE)*, 19(4), 2022, pp. 58-66.